doi:10.1093/brain/awv311 BRAIN 2016: 139; 62–72 | 62

BRAIN
A JOURNAL OF NEUROLOGY

Mutations in the *MORC2* gene cause axonal Charcot–Marie–Tooth disease

Teresa Sevilla,[1,2,3,*] Vincenzo Lupo,[2,4,*] Dolores Martínez-Rubio,[2,4] Paula Sancho,[2,4] Rafael Sivera,[1] María J. Chumillas,[2,5] Mar García-Romero,[6] Samuel I. Pascual-Pascual,[6] Nuria Muelas,[1,2] Joaquín Dopazo,[2,7] Juan J. Vílchez,[1,2,3] Francesc Palau,[2,4,8,#] and Carmen Espinós,[2,4,#]

[*,#]These authors contributed equally to this work.

Charcot–Marie–Tooth disease (CMT) is a complex disorder with wide genetic heterogeneity. Here we present a new axonal Charcot–Marie–Tooth disease form, associated with the gene microrchidia family CW-type zinc finger 2 (*MORC2*). Whole-exome sequencing in a family with autosomal dominant segregation identified the novel *MORC2* p.R190W change in four patients. Further mutational screening in our axonal Charcot–Marie–Tooth disease clinical series detected two additional sporadic cases, one patient who also carried the same *MORC2* p.R190W mutation and another patient that harboured a *MORC2* p.S25L mutation. Genetic and *in silico* studies strongly supported the pathogenicity of these sequence variants. The phenotype was variable and included patients with congenital or infantile onset, as well as others whose symptoms started in the second decade. The patients with early onset developed a spinal muscular atrophy-like picture, whereas in the later onset cases, the initial symptoms were cramps, distal weakness and sensory impairment. Weakness and atrophy progressed in a random and asymmetric fashion and involved limb girdle muscles, leading to a severe incapacity in adulthood. Sensory loss was always prominent and proportional to disease severity. Electrophysiological studies were consistent with an asymmetric axonal motor and sensory neuropathy, while fasciculations and myokymia were recorded rather frequently by needle electromyography. Sural nerve biopsy revealed pronounced multifocal depletion of myelinated fibres with some regenerative clusters and occasional small onion bulbs. *Morc2* is expressed in both axons and Schwann cells of mouse peripheral nerve. Different roles in biological processes have been described for MORC2. As the silencing of Charcot–Marie–Tooth disease genes have been associated with DNA damage response, it is tempting to speculate that a deregulation of this pathway may be linked to the axonal degeneration observed in *MORC2* neuropathy, thus adding a new pathogenic mechanism to the long list of causes of Charcot–Marie–Tooth disease.

1 Department of Neurology, Hospital Universitari i Politècnic La Fe, Avd. Fernando Abril Martorell no. 106, 46026 Valencia, Spain
2 Centro de Investigación Biomédica en Red de Enfermedades Raras (CIBERER), c/ Eduardo Primo Yúfera no. 13, 46012 Valencia, Spain
3 Department of Medicine, University of Valencia, Avd. Blasco Ibáñez no. 15, 46010 Valencia, Spain
4 Program in Rare and Genetic Diseases and IBV/CSIC Associated Unit, Centro de Investigación Príncipe Felipe (CIPF), c/ Eduardo Primo Yúfera no. 13, 46012 Valencia, Spain
5 Department of Clinical Neurophysiology, Hospital Universitari i Politècnic La Fe, Avd. Fernando Abril Martorell no. 106, 46026 Valencia, Spain
6 Department of Neuropaediatrics, Hospital Universitario La Paz, P° de la Castellana no. 261, 08046 Madrid, Spain
7 Program on Computational Genomics, Centro de Investigación Príncipe Felipe (CIPF), c/ Eduardo Primo Yúfera no. 13, 46012 Valencia, Spain

Received May 25, 2015. Revised September 8, 2015. Accepted September 8, 2015. Advance Access publication October 24, 2015

8 Department of Genetic and Molecular Medicine, and Pediatric Institute for Rare Diseases (IPER), Hospital Sant Joan de Déu, P° Sant Joan de Déu no. 2, 08950 Barcelona, Spain

Correspondence to: Dr Carmen Espinós,
Centro de Investigación Príncipe Felipe (CIPF),
Unit of Genetics and Genomics of Neuromuscular Diseases,
c/ Eduardo Primo Yúfera, 3. 46012 Valencia,
Spain
E-mail: cespinos@cipf.es

Keywords: Charcot-Marie-Tooth disease; *MORC2* gene; axonal degeneration; Schwann cell; whole-exome sequencing

Abbreviation: CMT = Charcot-Marie-Tooth disease

Introduction

The list of genes associated with Charcot–Marie–Tooth disease (CMT) and related-neuropathies is continually growing. More than 60 genes have been described (Neuromuscular Disease Center; http://neuromuscular.wustl.edu/time/hmsn.html), and about half of these CMT-associated genes were discovered after 2009 (Rossor *et al.*, 2013) due to the development of whole-exome sequencing using next generation sequencing. While more than 90% of patients with demyelinating CMT achieve an accurate molecular diagnosis, between 25–43% of axonal patients remain without a genetic diagnosis, even in the most recent clinical series (Saporta *et al.*, 2011; Murphy *et al.*, 2012; Sivera *et al.*, 2013; Fridman *et al.*, 2015). The identification of new genes involved in axonal CMT or CMT type 2 (CMT2) is critical to improve genetic diagnosis and also to gain insight into the pathophysiology of the disease.

CMT genes encode proteins that have a wide variety of roles, such as myelin structural proteins [PMP22, Cx32 (encoded by *GJB1*), MPZ], mitochondrial proteins (GDAP1, MFN2), enzymes involved in cellular trafficking [SBF1, MTMR13 (encoded by *SBF2*), MTMR2], aminoacyl tRNA synthetases (GARS, YARS, HARS, MARS, AARS), and others (Jerath and Shy, 2015). Shared cellular pathways can account for the convergence of different genes in similar phenotypes; likewise one gene may undertake distinct functions and its impairment can render divergent clinical pictures. The complexity of CMT can also be transferred to the clinical scenario, where the list of phenotypes is continuously growing and deep expertise is frequently required to handle diagnoses (Baets *et al.*, 2014; Harel and Lupski, 2014).

Using whole-exome sequencing we have identified mutations in the *MORC2* gene in CMT2 patients who presented either with generalized weakness in infancy, reminiscent of spinal muscular atrophy, or with an adult-onset asymmetric distal and proximal weakness with important sensory loss. This report adds a new piece to the puzzle of the genetics of CMT and contributes to a better understanding of the disease mechanisms.

Materials and methods

Patients

We investigated a CMT2 family (fCMT-237), belonging to our clinical series (Sivera *et al.*, 2013). Family fCMT-237 is a four-generation family with seven affected individuals with an autosomal dominant pattern of inheritance (Fig. 1A). In this family, mutations in CMT2 genes were previously ruled out (Sivera *et al.*, 2013). Further mutational screening of the *MORC2* gene in CMT2 families detected two additional affected individuals from Families fCMT-197 and fCMT-438 (Fig. 1A). In Family fCMT-197, also belonging to our clinical series, mutations in CMT2 genes were ruled out (Sivera *et al.*, 2013). In Family fCMT-438, mutations in *GDAP1*, *MFN2*, *GJB1*, *MPZ* and *IGHMBP2* genes, and the common *SMN1* deletion, were not detected. Clinical records were reviewed, and a new detailed neurological examination was carried out on affected and unaffected subjects. Nerve conduction studies were performed in seven affected and two unaffected individuals (Patients I:2 and III:2) from Family fCMT-237. Needle EMG studies were available in five patients (Patients II:3, III:1 and IV:3 from Family fCMT-237; Patient fCMT-197/II:4; and Patient fCMT-438/III:3). The electrophysiological studies were performed following a protocol described previously (Sevilla *et al.*, 2003). CMTNS2 (Charcot-Marie-Tooth neuropathy examination score 2) or CMTES2 (Charcot-Marie-Tooth examination score 2) was recorded in the last evaluation (Murphy *et al.*, 2011). Mean follow-up was 21 years. Sural nerve biopsy from two patients (Patients fCMT-237/III:1 and fCMT-197/II:4) was analysed using light and electron microscopy, as previously reported (Sevilla *et al.*, 2003). Muscular MRI was performed following a previously reported protocol (Sivera *et al.*, 2013).

Standard protocol approvals, registrations and patient consent

All patients and relatives included in the present study signed informed consent, and the research protocols were approved by the respective institutional board of the Ethics Committees of the corresponding Hospitals.

Genetic studies

Whole-exome sequencing was performed for DNA from four patients (Patients II:3, III:1, III:4 and IV:3; Fig. 1A) belonging

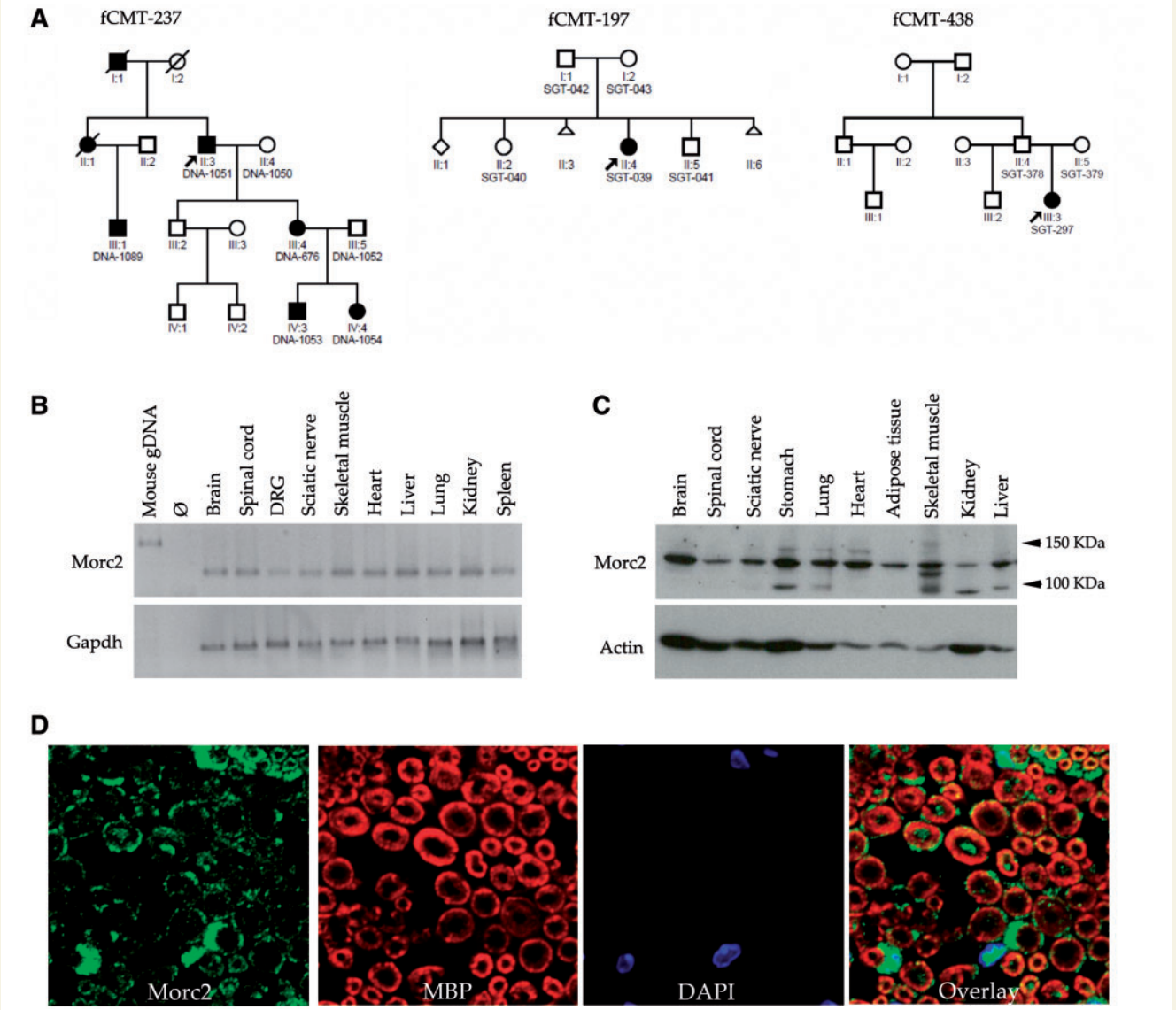

Figure 1 Families and analysis of Morc2 expression. (**A**) Pedigree of Families fCMT-237, fCMT-197 and fCMT-438. Available DNAs are indicated with the code DNA or SGT. (**B**) RT-PCR using a primer pair in exons 20 and 21, which amplified a 400 bp cDNA product. Mouse genomic DNA (gDNA) was used as positive control and to discard any genomic contamination for all samples tested. The mouse gDNA amplified product is 937 bp because 537 bp of the intron 20 are included. Ø = empty lane. (**C**) Immunoblot of MORC2 on protein extracts from neural and non-neural mouse tissues. (**D**) Immunostaining of MORC2 (green channel) and MBP (red channel) on a sciatic nerve cross-section. DAPI staining (blue) shows the Schwann cell nuclei.

to Family fCMT-237. Samples were subjected to exome enrichment with the Agilent SureSelect Human All Exon 50 Mb Kit followed by sequencing using the Illumina HiSeq 2000 Genome Analyzer platform at CNAG (Centro de Análisis Genómico, Barcelona, Spain). The data analysis was performed using the BIER platform pipeline (CIBERER) (Tort *et al.*, 2013). Then, we selected all heterozygous nucleotide changes shared among all four affected individuals. To filter out common single nucleotide polymorphisms (SNPs) and indels with allele frequency cut-offs at 0.01%, we used following database: dbSNP (http://www.ncbi.nlm.nih.gov/SNP), ESP6500 (http://evs.gs.washington.edu/EVS/), ExAC (http://exac.broadinstitute.org/), and CSVS (http://csvs.babelomics.org/). Finally, novel changes were first selected as candidate variants, and further validated by Sanger sequencing on a 96-capillary Applied Biosystems 3730xl DNA Analyzer.

The variants with uncertain significance were further investigated by segregation analysis in the seven available DNAs from Family fCMT-237 (Fig. 1A). The Clustal Omega software (http://www.ebi.ac.uk/Tools/msa/clustalo/) was used to investigate the conservation of the candidate changes. The biological relevance of the novel amino acid changes was studied using both SIFT (http://blocks.fhcrc.org/sift/SIFT.html) and PolyPhen-2 (http://genetics.bwh.harvard.edu/pph2/index.shtml) programs.

A search for mutations using Sanger sequencing of the codified regions of the *MORC2* gene was performed in 52 unrelated CMT2 families with no genetic diagnosis. All primers

and PCR conditions are available upon request. For Family fCMT-438, *SMN1* genetic testing for the common *SMN1* deletion was performed as described previously (van der Steege *et al.*, 1995), and gene dosage analysis was investigated with multiplex ligation-dependent probe amplification (MLPA) using the SALSA MLPA P021 (version A2) (MRC-Holland, Amsterdam, The Netherlands).

Gene expression

Total RNA from several adult mice tissues was isolated using TriPure isolation reagent (Roche Applied Science). A 400 bp cDNA fragment of *Morc2* between exon 20–21 was amplified by reverse transcriptase-polymerase chain reaction (RT-PCR). Sciatic nerve protein extract was obtained from mice using a polytron homogenizer and lysis buffer (50 mM Tris-HCl pH 7.4, 5 mM DTT, 150 mM NaCl, 1% NP-40, 0.5% deoxycolate). To evaluate histological expression of *Morc2* in peripheral nerves, mice sciatic nerves were dissected and post-fixed by immersion in 4% paraformaldehyde. Fifteen-micrometre cross-sections were immunostained and mounted in DAPI Fluoromount-G® (Southern Biotech). Images were visualized using a Leica TCS SP2 confocal system.

A rabbit polyclonal α-MORC2 antibody (Santa Cruz Biotechnology; used at 1:500) was used to perform both immunoblotting and immunofluorescence studies. In addition, a second rabbit polyclonal α-MORC2 antibody (Bioss Inc.; used at 1:500) was used to validate the immunofluorescence results. A rat monoclonal myelin basic protein (MBP) antibody (Abcam; used at 1:1000) was used as a compact myelin marker. To detect α-MORC2 and α-MBP, Alexa Fluor® 448-conjugated goat anti-rabbit IgG and Alexa Fluor® 647-conjugated goat anti-rat IgG antibodies (Thermo Fisher Scientific; both at 1:500) were used, respectively.

Results

Clinical picture

The clinical characteristics are summarized in Table 1. Patients belonging to Family fCMT-237 experienced their first symptom in childhood or early adulthood, while Family fCMT-197's proband reported a delay in the acquisition of motor milestones. The most frequent initial symptom was cramps in the lower limbs, and all affected individuals showed distal lower limb weakness and sensory loss during the initial examination. Hand weakness appeared after distal lower limbs paresis in most patients.

Proximal involvement was very frequent in the later stages of the disease, including neck flexion weakness in four patients (Table 1). At the time of the last examination, the older patients presented prominent asymmetric pelvic and shoulder girdle muscle weakness with relative sparing of knee and elbow extension (score of 3 or 4 on the Medical Research Council scale) even in the most severely affected patients (Supplementary Fig. 1). Two of them required an electric wheelchair for mobility, and also had significant disability of the upper limbs. Tendon reflexes were absent in all patients except for the two youngest (Patients fCMT-237/IV:3 and IV:4). All had pes cavus, and the more severely affected patients (CMTNS2 > 20) showed scoliosis as well. Sensory loss was observed in all cases, being more remarkable in older patients. The two most severely patients (Patients fCMT-237/II:3 and fCMT-197/II:4) complained of urinary incontinence; Patient fCMT-237/II:3 had undergone urodynamic evaluation that revealed absent detrusor contractility.

Family fCMT-438's proband presented with hypotonia and muscle weakness at birth after a normal pregnancy and delivery. She achieved unstable passive sedestation at 6 months, but neither active sedestation nor independent bipedestation were possible at 17 months. On examination, she had microcephaly (cranial perimeter below third percentile), generalized weakness including slight facial involvement and generalized areflexia. Cognitive and language development was normal. Brain MRI showed unspecific mild dismaturative features. She was re-examined at 19 months of age and showed a slight improvement.

Electrophysiological studies (Table 2) showed normal or near normal motor nerve conduction velocities in almost all nerves, while the compound muscle action potentials showed widespread decreased amplitude in a noticeable asymmetrical fashion; upper limb nerves were less severely affected. Sensory nerve action potentials showed low amplitude or were unobtainable. Needle EMG revealed chronic neurogenic changes and prominent spontaneous activity at rest composed of fasciculations and myokymia, activated or increased with muscle contraction. This activity was recorded in both distal and proximal muscles.

Muscular MRI was performed in two patients (Patients fCMT-237/III:4 and fCMT-197/II:4) (Fig. 2). In Patient fCMT-237/III:4, intrinsic muscles of the feet showed a loss of volume and pockets of fat infiltration with relative preservation of interossei and flexor foot muscles. In the legs there was relative preservation of bilateral deep posterior compartment muscles, whereas the remaining muscles in the anterolateral and outer posterior compartments were fully replaced by fat. In the thighs there was a moderate fat infiltration of the quadriceps, and the posterior and medial thigh musculature. Pelvic muscles showed moderate atrophy with little fat infiltration. In Patient fCMT-197/II:4, the muscles in the feet and legs were almost completely replaced by fat, and there was high fat infiltration in the muscles of the thighs and pelvis. In the arms there was also marked fatty substitution in all muscles, and in the shoulder, the deltoid muscle was completely replaced by fat while the periscapular muscles were relatively preserved.

Sural nerve biopsy

The two nerve biopsies analysed revealed similar pathological findings (Fig. 3). Semi-thin sections showed a pronounced depletion of myelinated fibres. Fibre density was 3837/mm^2 in Patient fCMT-237/II:3, 1650/mm^2 in Patient fCMT-197/II:4, and 7950/mm^2 in the control subject. The histogram confirmed a predominant loss of large

Table 1 Clinical data at first and last evaluation

Family Patient	Sex	Onset	First evaluation				Last evaluation					
			Age	LL weakness Prox/Dist	UL weakness Prox/Dist	Sensory loss	Age	LL weakness Prox/Dist	UL weakness Prox/Dist	Sensory loss	Other CMTNS2	Functional status
fCMT-237 II:1	F	?[a] Worsening weakness in UL and LL weakness	41 yo	+ +/+ + +	+ + +/+ + +	P, V, T		No follow up	No follow up	P, V, T	Poliomyelitis	Dead at 69
fCMT-237 II:3	M	4–5 yo Walking awkwardly	38 yo	–/+ +	–/+ +	P, V	75 yo	+ + +/+ + +	+ + +/+ + +	All in LL P, V, T in UL	Hearing loss Neck weakness 31	Electric wheelchair Just move right hand
fCMT-237 III:1	M	Infancy Walking awkwardly	11 yo	–/+	–/–	P	47 yo	+/+ + +	+/+ +	P, V, T	24	Needs a cane
fCMT-237 III:4	F	14 yo, LL weakness 20 yo, UL weakness	15 yo	+ +	+	P, V, T	51 yo	+/+ + +	+/+ + +	P, V, T	Hearing loss Neck weakness 27	Needs a cane Claw hands
fCMT-237 IV:3	M	5 yo Walking awkwardly	12 yo	–/+	–/+	V	20 yo	–/+	–/+	V	Neck weakness 11	He can't stand on heels Cramps, especially in hands
fCMT-237 IV:4	F	Asymptomatic	9 yo	–/+	–/–	V	17 yo	–/+	–/–	V	CMTES2[b] = 4	She can't stand on heels
fCMT-197 II:4	F	18 mo Delayed walking	22 yo	–/+ +	–/+	P, V	45 yo	+ + +/+ + +	+ + +/+ + +	P, V, T	Neck weakness 32	Claw hands Electric wheelchair
fCMT-438 III:3	F	<6 mo Generalized hypotonia and weakness	17 mo	+ + +	+ + +	unknown	19 mo	+ + +	+ + +	Unknown	NA	No active trunk sitting

F = female; M = male; LL = lower limb; UL = upper limb; Prox. = proximal; Dist. = distal; + = mild distal weakness; ++ = moderate distal weakness; + + + = severe distal weakness or proximal involvement; P = pinprick; V = vibratory; T = Touch; NA = not applicable. [a]Difficult to determine due to poliomyelitis in infancy. [b]CMTES was determined because electrophysiological studies at last examination were not available.

Table 2 Electrophysiological studies

Family Patient	Age	Motor nerve conductions					Sensory nerve conductions				
		Median (CMAP/CV)	Ulnar (CMAP/CV)	Axillar (CMAP)	Tibial (CMAP/CV)	Peroneal (CMAP/CV)	Median (SNAP/CV)	Ulnar (SNAP/CV)	Radial (SNAP/CV)	Sup. peroneal (SNAP/CV)	Sural (SNAP/CV)
fCMT-237 II:1	41 yo	–	–	–	–	NR	–	–	–	–	NR
fCMT-237 II:3	75 yo	–	4.5 mV 58.3 m/s	2.3 mV	–	NR	–	–	1.2 µV 55.2 m/s	NR	NR
fCMT-237 III:1	47 yo	7.8 mV 53.3 m/s	10.2 mV 61.7 m/s	3.2 mV	13.4 mV 47.6 m/s	0.7 mV 43.3 m/s	NR	NR	3.1 µV 53.6 m/s	NR	NR
fCMT-237 III:4	51 yo	2.2 mV[a]	4.3 mV 58 m/s	10.6 mV	5.2 mV 42.5 m/s	2.3 mV 37.3 m/s	–	–	5.6 µV 53.3 m/s	–	NR
fCMT-237 IV:3	20 yo	6.6 mV[a]	8.2 mV 54.7 m/s	19.4 mV	10.3 mV 50.0 m/s	3.5 mV 46.8 m/s	–	3.1 µV 53.6 m/s	6.9 µV 53.4 m/s	NR	1.2 µV 51.9 m/s
fCMT-197 II:4	45 yo	1 mV 50 m/s	3 mV 50 m/s	4 mV	0.1 mV	NR	NR	NR	NR	–	NR
fCMT-438 III:3	17 mo	–	–	–	–	0.7 mV 31.7 m/s	–	–	–	–	3.3 µV 53.8 m/s

Sup. = superficial; CMAP = compound muscle action potential; SNAP = sensory nerve action potential; CV = conduction velocity; NR = not recordable. [a]Median and ulnar physiological anastomosis.

diameter fibres with relative preservation or even an increase in small fibres (<6 µm). Fibre loss was unevenly distributed, giving the appearance of a multifocal profile like that observed in ischaemic neuropathies. Occasional small onion bulbs and variable presence of regenerative clusters were visible. There were no abnormalities in the shape or compaction of myelin sheaths, although a number of myelin sheaths appeared disproportionally thinly myelinated. Active axonal degeneration was rarely observed, and the majority fibres presented a normal axonal compartment without alterations in mitochondria and tubule-filamentous elements. By simple inspection, disregarding unmyelinated axons associated with onion bulbs and regenerative clusters, the unmyelinated fibre populations presented normal shape but seemed to be reduced in number. In the intrafascicular compartment there were areas of fibrosis where the only cellular elements remaining were flattened Schwann cell processes embedded in dense collagen deposits.

Genetic analyses

Capture of our whole-exome sequencing was performed with a uniform coverage; for all four samples from Family fCMT-237, the mean coverage was 84.43, and the standard deviation coverage was 73.77. Filtering data revealed 52 nucleotide changes in heterozygosis shared among all four patients, compatible with a dominant inheritance, and a minor allele frequency < 1%. Out of the 52, seven variants were novel (Supplementary Table 1). Segregation analysis of the seven available DNAs (Fig. 1A) ruled out all of them, except the heterozygous c.568C > T change in the *MORC2* gene (NM_014941.1), which is predicted to cause the amino acid substitution p.R190W (NP_055756.1). The screening of c.568C > T in 212 healthy controls of matched geographical ancestry did not show this genetic variant. Next, we performed a mutational screening in 52 undiagnosed CMT2 families. Two additional probands carrying *MORC2* mutations were identified. The proband from Family fCMT-197 harbours the same *MORC2* c.568C > T change in heterozygosis and Family fCMT-438's proband is a heterozygous carrier of the novel *MORC2* c.74C > T (p.S25L) mutation. Both mutated nucleotides, c.568C > T and c.74C > T, are part of a CpG-sequence. False paternity was excluded for both patients (data not shown), supporting that mutations occur *de novo* in Families fCMT-197 and fCMT-438 (Fig. 1A).

The computational analyses revealed that the R190 and S25 residues are evolutionarily conserved amino acids. The pathogenicity prediction indicates that both p.R190W and p.S25L are likely damaging, with a SIFT score of 0.0 and a PolyPhen-2 score of 1.0 for each change. Both p.R190W and p.S25L mutations are localized in the GHL (Gyrase B, Hsp90, and MutL)-ATPase domain of the protein MORC2 (Supplementary Fig. 2).

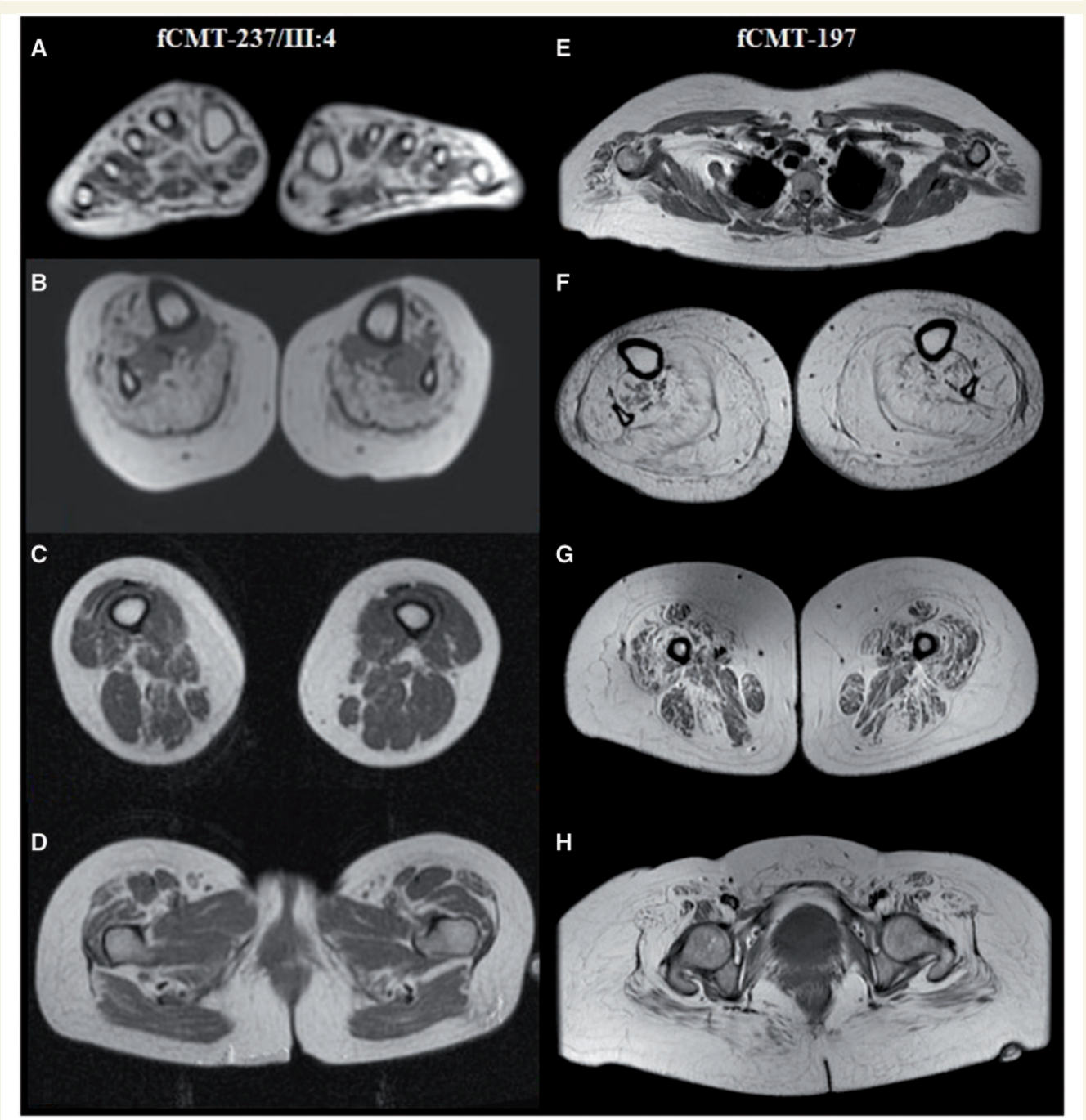

Figure 2 Axial T_1-weighted MRI scans from Patients fCMT-237/III:4 and fCMT-197/II:4. The scans were obtained for the foot (**A**), calf (**B** and **F**), thigh (**C** and **G**), pelvis (**D** and **H**) and scapular girdle at the level Th4 (**E**). MRI findings correspond well with the clinical phenotype. In the patient with a less severe clinical phenotype, fatty replacement is more apparent in muscles of the calf, with preservation seen only in the deep posterior compartment muscles (**B**). The intrinsic foot muscles, flexors and interossei muscles are relatively preserved (**A**). Muscles of the thigh (**C**) and pelvis (**D**) show mild fatty degeneration and atrophy. In the patient with a more severe clinical phenotype, an almost diffuse involvement can be observed in calf (**F**), thigh (**G**) and pelvis muscles (**H**). Atrophy of periscapular muscles and prominent fatty replacement in the shoulder muscle are present, particularly in the posterior portion of the deltoid (**E**).

Gene expression

Analysis of cDNA from total RNA obtained from several mice tissues showed that *Morc2* is ubiquitously expressed (Fig. 1B). To better establish whether mouse *Morc2* is expressed in the peripheral nervous system, we performed western blot analysis and immunofluorescence assay using protein extracts and cross-sections of sciatic nerve, respectively. In the western blot, we observed a band with an

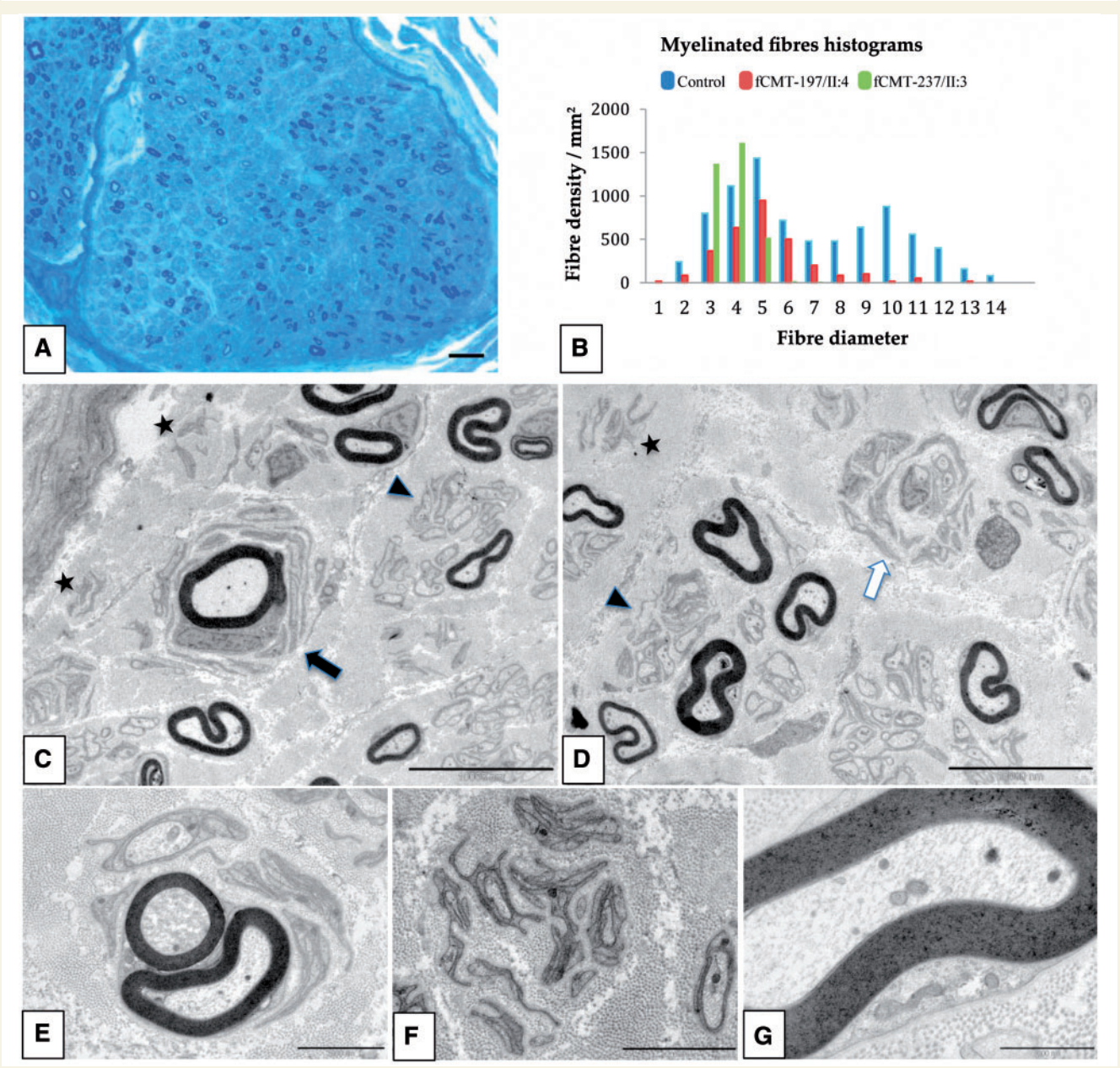

Figure 3 Distal sural nerve biopsy. (**A**) Transverse semi-thin section revealing a depletion of myelinated fibres in an uneven patchy pattern. (**B**) Myelinated fibre histogram showing a predominant loss of large myelinated fibres. Electron microscope micrographs in a low power view show (**C** and **D**) a few remaining small myelinated fibres and an occasional onion bulb enclosing a myelinated axon (black arrow) or unmyelinated axons (white arrow). Note the presence of a regenerative cluster (arrowhead) and assemblies of flattened Schwann cell processes devoid of axons embedded in collagen (asterisk). Details at higher magnification of different regenerative cluster types composed of small myelinated and unmyelinated axons (**E**) or including stacked Schwann cell processes reminiscent of Bügner bands showing declining features (**F**). (**G**) A magnified myelinated fibre with proper myelin compaction and normal appearance of axoplasmic organelles and adjacent Schwann cell components. Scale bars: **A** = 20 μm; **C** and **D** = 10 μm; **E** to **G** = 2 μm.

estimated size of 117 kDa, corresponding to MORC2 for all the neural and non-neural tissues (Fig. 1C). In some of the non-neural tissues were detected additional bands. Confocal images of sciatic nerve in cross-section revealed that MORC2 is localized in both axons and Schwann cells (Fig. 1D).

Discussion

We have identified two different mutations in the *MORC2* gene in patients from three unrelated families presenting with an axonal motor and sensory neuropathy. This gene has not been previously linked to neuropathies. Although

the clinical series includes only eight cases, the prompt evaluation of early-onset patients and the long lasting follow up of many of these patients allows us to depict the clinical profile, which includes aspects that exceed the classic CMT2 phenotype.

The onset of the symptoms in Family fCMT-237 varied from early childhood to young adulthood and the majority of cases reported cramps and distal lower limb symptoms. However, over the course of years, weakness spread to upper limbs and girdle muscles in an asymmetric fashion without following a homogenous distal to proximal gradient. Progression was not strictly length dependent, as can be confirmed by the MRI of Patient fCMT-237/III:4, where there is a relative preservation of the intrinsic foot muscles, and a complete fatty substitution of all the muscles in the calves except for the tibialis posterior. This morphological pattern contrasts with the classic progression in other CMT phenotypes, such as *PMP22* duplication and *MFN2*- or *GDAP1*-related neuropathies, where when the muscles of thighs are affected, there is already complete fatty substitution of the muscles of the feet (Gallardo *et al.*, 2006; Chung *et al.*, 2008; Sivera *et al.*, 2010). Sensory nerve involvement developed early in the disease course, and could already be detected in Family fCMT-237's younger patients. Clinical and/or electrophysiological progression of sensory impairment could be traced in several cases. During the whole disease course, there were prominent positive motor symptoms (cramps, etc.) with an electrical correlate of myokymia and fasciculations in EMG.

Interestingly, the two sporadic patients presented a congenital or infantile onset developing hypotonia, generalized weakness, and delay of the acquisition of motor milestones. The fCMT-438/III:3 patient was reminiscent of spinal muscular atrophy, but with a clear concomitant sensory impairment in nerve conduction studies. The natural history of the patient could not be recorded, as follow-up only reached up to 19 months. In Patient fCMT-197/II:4, once the delayed maturational period ended, a degenerative stage ensued similar to that observed in members of Family fCMT-237. Infantile spinal muscular atrophy-like syndromes have been associated with mutations in the *TRPV4* gene but *MORC2* patients diverged with respect to concomitant sensory impairment and were absent of arthrogryposis (Echaniz-Laguna *et al.*, 2014).

As with *MORC2* neuropathy, there are other forms of hereditary neuropathies that can also present with localized or widespread muscle weakness not respecting the ascending progression characteristic of axonal degeneration in CMT. Vulnerability of specific motor neurons populations has been associated with thenar atrophy in *GARS* (Antonellis *et al.*, 2003), infantile lower extremities in *DYNC1H1* (Harms *et al.*, 2012), vocal cord and scapulaperoneal affectation in *TRPV4* (Zimon *et al.*, 2010), lower limbs in *DNAJB2* (Blumen *et al.*, 2012), calf muscles in *FBXO38* (Sumner *et al.*, 2013) and proximal involvement in *TFG* (Ishiura *et al.*, 2012) genes. However, most of the aforementioned pictures correspond to purely motor phenotypes, and in MORC2 there is an early and significant sensory impairment that was substantiated in nerve conduction studies and sural nerve biopsies. In the latter, the findings were consistent with a typical axonal neuropathy with similar features to those observed in typical axonopathies such as *MFN2* (Chung *et al.*, 2006) and *GDAP1* (Sevilla *et al.*, 2003) neuropathies. The only specific *MORC2* pathological feature was the multifocal pattern of myelinated fibre loss, which could explain the different degrees of axonal vulnerability and is consistent with the asymmetric and random-like pattern of muscle weakness.

We have demonstrated that *Morc2* is expressed in both axons and Schwann cells of mouse peripheral nerve. Microrchidia family CW-type zinc finger 2 (MORC2) is a member of the MORC protein family (Inoue *et al.*, 1999; Iyer *et al.*, 2008), which is conserved in higher eukaryotes, suggesting that this protein family has relevant biological functions in organisms. Four MORC proteins have been predicted in humans (MORC1 to MORC4), which share four domains, a GHL-ATPase domain at the amino-terminus, a CW-type zinc finger domain, a nuclear localization signal, and coiled-coil domains at the carboxy-terminus. The two identified mutations in our families are placed in the ATPase domain, suggesting that this activity could be altered in the protein.

MORC2 has been postulated to be a transcriptional gene repressor in cancer cells, specifically for gastric cancer (Shao *et al.*, 2010; Wang *et al.*, 2010). Moreover, MORC2 phosphorylation seems to be involved in promoting gastric cell proliferation (Wang *et al.*, 2015), and interacts with ATP-citrate lyase, an enzyme that catalyses the formation of acetyl-CoA. In addition MORC2 plays a role in lipogenesis and adipogenesis (Sánchez-Solana *et al.*, 2014), and is a substrate of PAK1 (p21-activated kinase 1), an integrator of extracellular signals and nuclear processes (Li *et al.*, 2012). After DNA damage, PAK1 phosphorylates MORC2 on serine 739, facilitates an ATPase-dependent chromatin relaxation and promotes the induction of the phosphorylation of the histone H2AX (γ-H2AX). In a genome-wide siRNA screen, 22 genes involved in CMT have increased γ-H2AX levels, an early mark of DNA damage (Paulsen *et al.*, 2009), suggesting a connection between CMT and the DNA damage response. Although it is tempting to speculate that the neuropathy in these *MORC2* patients is linked to DNA damage response, other pathomechanistic pathways may certainly be involved.

In conclusion, *MORC2* mutations are responsible for an axonal motor and sensory neuropathy with a congenital or infantile onset presenting as a spinal muscular atrophy-like picture, and with a childhood or juvenile onset that starts distally and progresses to involve proximal muscles in an asymmetric and random fashion causing severe disability in adults. Significant positive motor activity such as cramps, fasciculations and myokymia are present from the beginning. A deregulation of the DNA damage response

pathway may be responsible for axonal degeneration in *MORC2* neuropathy, thus adding a new pathogenic mechanism to the long list of causes of CMT.

Acknowledgements

We deeply appreciate the commitment of the families studied. We are grateful to Dr Consuelo Guerri and her team at the CIPF for providing us some antibodies. The authors wish to thank Microscopy Units from UPV and IIS La Fe for their technical support.

Funding

This collaborative joint project is awarded by IRDiRC and funded by the Instituto de Salud Carlos III (ISCIII) - Subdirección General de Evaluación y Fomento de la Investigación within the framework of the National R+D+I Plan (IR11/TREAT-CMT to T.S., S.I.P.P., F.P. and C.E.; PI12/00453 to C.E.; and PI12/0946 to T.S.), co-funded with FEDER funds. Additional support was provided by the Ramón Areces Foundation and by the ISCIII and the Centro de Investigación Príncipe Felipe (CPII14/00002) to C.E.

Supplementary material

Supplementary material is available at *Brain* online.

References

Antonellis A, Ellsworth RE, Sambuughin N, Puls I, Abel A, Lee-Lin SQ, et al. Glycyl tRNA synthetase mutations in Charcot-Marie-Tooth disease type 2D and distal spinal muscular atrophy type V. Am J Hum Genet 2003; 72: 1293–9.

Baets J, De Jonghe P, Timmerman V. Recent advances in Charcot-Marie-Tooth disease. Curr Opin Neurol 2014; 27: 532–40.

Blumen SC, Astord S, Robin V, Vignaud L, Toumi N, Cieslik A, et al. A rare recessive distal hereditary motor neuropathy with HSJ1 chaperone mutation. Ann Neurol 2012; 71: 509–19.

Chung KW, Kim SB, Park KD, Choi KG, Lee JH, Eun HW, et al. Early onset severe and late-onset mild Charcot-Marie-Tooth disease with mitofusin 2 (MFN2) mutations. Brain 2006; 129: 2103–18.

Chung KW, Suh BC, Shy ME, Cho SY, Yoo JH, Park SW, et al. Different clinical and magnetic resonance imaging features between Charcot-Marie-Tooth disease type 1A and 2A. Neuromuscul Disord 2008; 18: 610–18.

Echaniz-Laguna A, Dubourg O, Carlier P, Carlier RY, Sabouraud P, Pereon Y, et al. Phenotypic spectrum and incidence of TRPV4 mutations in patients with inherited axonal neuropathy. Neurology 2014; 82: 1919–26.

Fridman V, Bundy B, Reilly MM, Pareyson D, Bacon C, Burns J, et al. CMT subtypes and disease burden in patients enrolled in the Inherited Neuropathies Consortium natural history study: a cross-sectional analysis. J Neurol Neurosurg Psychiatry 2015; 86: 873–8.

Gallardo E, Garcia A, Combarros O, Berciano J. Charcot-Marie-Tooth disease type 1A duplication: spectrum of clinical and magnetic resonance imaging features in leg and foot muscles. Brain 2006; 129: 426–37.

Harel T, Lupski JR. Charcot-Marie-Tooth disease and pathways to molecular based therapies. Clin Genet 2014; 86: 422–31.

Harms MB, Ori-McKenney KM, Scoto M, Tuck EP, Bell S, Ma D, et al. Mutations in the tail domain of DYNC1H1 cause dominant spinal muscular atrophy. Neurology 2012; 78: 1714–20.

Inoue N, Hess KD, Moreadith RW, Richardson LL, Handel MA, Watson ML, et al. New gene family defined by MORC, a nuclear protein required for mouse spermatogenesis. Hum Mol Genet 1999; 8: 1201–7.

Ishiura H, Sako W, Yoshida M, Kawarai T, Tanabe O, GotAhsan B, et al. The TRK-fused gene is mutated in hereditary motor and sensory neuropathy with proximal dominant involvement. Am J Hum Genet 2012; 91: 320–9.

Iyer LM, Abhiman S, Aravind L. MutL homologs in restriction-modification systems and the origin of eukaryotic MORC ATPases. Biol Direct 2008; 3: 8.

Jerath NU, Shy ME. Hereditary motor and sensory neuropathies: understanding molecular pathogenesis could lead to future treatment strategies. Biochim Biophys Acta 2015; 1852: 667–78.

Li DQ, Nair SS, Ohshiro K, Kumar A, Nair VS, Pakala SB, et al. MORC2 signaling integrates phosphorylation-dependent, ATPase-coupled chromatin remodeling during the DNA damage response. Cell Rep 2012; 2: 1657–69.

Murphy SM, Herrmann DN, McDermott MP, Scherer SS, Shy ME, Reilly MM, et al. Reliability of the CMT neuropathy score (second version) in Charcot-Marie-Tooth disease. J Peripher Nerv Syst 2011; 16: 191–8.

Murphy SM, Laura M, Fawcett K, Pandraud A, Liu YT, Davidson GL, et al. Charcot-Marie-Tooth disease: frequency of genetic subtypes and guidelines for genetic testing. J Neurol Neurosurg Psychiatry 2012; 83: 706–10.

Paulsen RD, Soni DV, Wollman R, Hahn AT, Yee MC, Guan A, et al. A genome-wide siRNA screen reveals diverse cellular processes and pathways that mediate genome stability. Mol Cell 2009; 35: 228–39.

Rossor AM, Polke JM, Houlden H, Reilly MM. Clinical implications of genetic advances in Charcot-Marie-Tooth disease. Nat Rev Neurol 2013; 9: 562–71.

Sánchez-Solana B, Li DQ, Kumar R. Cytosolic functions of MORC2 in lipogenesis and adipogenesis. Biochim Biophys Acta 2014; 1843: 316–26.

Saporta AS, Sottile SL, Miller LJ, Feely SM, Siskind CE, Shy ME. Charcot-Marie-Tooth disease subtypes and genetic testing strategies. Ann Neurol 2011; 69: 22–33.

Sevilla T, Cuesta A, Chumillas MJ, Mayordomo F, Pedrola L, Palau F, et al. Clinical, electrophysiological and morphological findings of Charcot-Marie-Tooth neuropathy with vocal cord palsy and mutations in the GDAP1 gene. Brain 2003; 126: 2023–33.

Shao Y, Li Y, Zhang J, Liu D, Liu F, Zhao Y, et al. Involvement of histone deacetylation in MORC2-mediated down-regulation of carbonic anhydrase IX. Nucleic Acids Res 2010; 38: 2813–24.

Sivera R, Espinós C, Vilchez JJ, Mas F, Martinez-Rubio D, Chumillas MJ, et al. Phenotypical features of the p.R120W mutation in the GDAP1 gene causing autosomal dominant Charcot-Marie-Tooth disease. J Peripher Nerv Syst 2010; 15: 334–44.

Sivera R, Sevilla T, Vilchez JJ, Martinez-Rubio D, Chumillas MJ, Vazquez JF, et al. Charcot-Marie-Tooth disease: genetic and clinical spectrum in a Spanish clinical series. Neurology 2013; 81: 1617–25.

Sumner CJ, d'Ydewalle C, Wooley J, Fawcett KA, Hernandez D, Gardiner AR, et al. A dominant mutation in FBXO38 causes distal spinal muscular atrophy with calf predominance. Am J Hum Genet 2013; 93: 976–83.

Tort F, Garcia-Silva MT, Ferrer-Cortes X, Navarro-Sastre A, Garcia-Villoria J, Coll MJ, et al. Exome sequencing identifies a new mutation in SERAC1 in a patient with 3-methylglutaconic aciduria. Mol Genet Metab 2013; 110: 73–7.

van der Steege G, Grootscholten PM, van der Vlies P, Draaijers TG, Osinga J, Cobben JM, et al. PCR-based DNA test to confirm clinical diagnosis of autosomal recessive spinal muscular atrophy. Lancet 1995; 345: 985–6.

Wang G, Song Y, Liu T, Wang C, Zhang Q, Liu F, et al. PAK1-mediated MORC2 phosphorylation promotes gastric tumorigenesis. Oncotarget 2015; 6: 9877–86.

Wang GL, Wang CY, Cai XZ, Chen W, Wang XH, Li F. Identification and expression analysis of a novel CW-type zinc finger protein MORC2 in cancer cells. Anat Rec (Hoboken) 2010; 293: 1002–9.

Zimon M, Baets J, Auer-Grumbach M, Berciano J, Garcia A, Lopez-Laso E, et al. Dominant mutations in the cation channel gene transient receptor potential vanilloid 4 cause an unusual spectrum of neuropathies. Brain 2010; 133: 1798–809.